

Article

# Influence of Powertrain Topology and Electric Machine Design on Efficiency of Battery Electric Trucks—A Simulative Case-Study

Sebastian Wolff \*, Svenja Kalt , Manuel Bstieler and Markus Lienkamp

Institute of Automotive Technology, Technical University of Munich, 85748 Garching b. München, Germany; kalt@ftm.mw.tum.de (S.K.); manuel.bstieler@tum.de (M.B.); lienkamp@ftm.mw.tum.de (M.L.)

\* Correspondence: sebastian.wolff@tum.de

**Abstract:** The advancement of electric mobility as a measure to comply with international climate targets and sustain renewable resources in the future has led to an electrification of the mobility sector in recent years. This trend has not been spared in the logistics and commercial vehicle sector. Emerging electric powertrain concepts for long-haul vehicles have since been developed and adapted to different use cases and axle concepts. In this paper, the authors show the influence of the powertrain topology and the associated design of the electric machine on the efficiency and energy consumption of commercial vehicles. For this, existing series or prototype long-haul axle topologies are analyzed regarding their efficiency and operating points within four driving cycles. Additionally, a sensitivity analysis on the influence of the total gearbox ratio tests the assumed designs. We find that single-machine topologies offer efficiency advantages over multiple-machine topologies. However, this study highlights a joint consideration of application-specific machine design and topology to realize the full technological potential.

**Keywords:** battery electric; heavy-duty trucks; electric machines; powertrain design; topology; efficiency



**Citation:** Wolff, S.; Kalt, S.; Bstieler, M.; Lienkamp, M. Influence of Powertrain Topology and Electric Machine Design on Efficiency of Battery Electric Trucks—A Simulative Case-Study. *Energies* **2021**, *14*, 328. <https://doi.org/10.3390/en14020328>

Received: 21 December 2020

Accepted: 7 January 2021

Published: 8 January 2021

**Publisher's Note:** MDPI stays neutral with regard to jurisdictional claims in published maps and institutional affiliations.



**Copyright:** © 2021 by the authors. Licensee MDPI, Basel, Switzerland. This article is an open access article distributed under the terms and conditions of the Creative Commons Attribution (CC BY) license (<https://creativecommons.org/licenses/by/4.0/>).

## 1. Introduction

With the Paris Agreement, not only the European Union (EU) but 189 countries in total, pledged to reduce greenhouse gases and limit global warming to 1.5–2 °C [1]. Therefore, the EU set goals to reduce total greenhouse gas emissions by 40% until 2030 and by at least 80% by 2050 compared to the levels of 1990.

Transportation, and road transportation in particular, is the backbone of our economy. However, transportation also accounts for 27% of European greenhouse emissions, of which road transport comprises 72% [2]. Road transportation consequently provides large leverage to achieve the ambitious climate goals of the Paris Agreement. Consequently, the EU introduced CO<sub>2</sub> limits for medium- and heavy-duty vehicles in 2019 to reduce emissions by 15% in 2025 and 30% in 2030 compared to 2019 levels [3].

Rising environmental responsibility is one among other push factors towards electromobility. Rising energy as well as the dependency of fossil oil and gas promote the transformation of today's transportation systems [4,5]. However, electromobility refers to different vehicle concepts such as hybrid (HEV), battery electric (BEV), and fuel-cell-electric vehicles (FCEV), whereby the latter two enable locally emission-free driving. In addition, the electric powertrains offer superior start-up torque and efficiency compared to conventional internal combustion engine vehicles (ICEV) [4–6].

Regulations and technical development have created the potential for the application of battery electric trucks in long-distance transportation. Currently, different concepts for the electrification of heavy-duty trucks exist. However, it is not yet decided which vehicle concept provides an optimal solution fulfilling long-haul requirements [7]. In this paper, we show the influence of the topology choice and the associated design of the electric

machine (EM) on the efficiency and energy consumption of commercial vehicles. We use simulation tools to obtain the machine designs and efficiencies for five powertrain concepts in series or prototype state.

The essential components of a powertrain are the electric machine, the inverter, and the battery. However, the optimization of the electric machine efficiency promises improvements because its efficiency is currently lower than the remaining components.

In particular, the machine efficiency depends on its loads. Thus the application in a wide range of operating points requires further optimization of the machine design (power, weight, and size) to maximize the efficiency [8]. Therefore, this study neglects the potential of battery or additional component optimization and focuses on the effect of the powertrain topology combined with electric machine design.

### 1.1. Battery Electric Heavy-Duty Trucks

Long-haul trucks have three major requirements: high efficiency, high payload and long range. Due to current developments in the automotive industry, commercial vehicles also benefit from advances in battery and powertrain technology. This enables battery electric vehicles to potentially fulfill the requirements of long-haul transportation [4,6,9,10]. Due to their high mileage, efficiency is a major requirement for trucks. The limitation of range and the reduction of payload, however, require BEV trucks to rate efficiency even higher.

Long-haul vehicles typically have one ( $4 \times 2$ ) or two ( $6 \times 4$ ) driven axles, although the majority of European vehicles are single-axle [11,12]. Current internal combustion engine (ICE)-powered vehicles have transmissions of up to 16 gears and a rear axle differential (final drive) to achieve the best possible utilization of the tractive force [12,13].

Battery electric vehicles offer new possibilities to design heavy-duty vehicle concepts and powertrains. Because electric machines are smaller than equivalent ICE, their position in the vehicle package is more flexible. Additionally, the EM torque characteristics allow for reduced gears or even a fixed gear ratio.

Verbruggen et al. [14] categorize electric powertrain topologies by three design choices: central or distributed drive, fixed or multiple gears, and the number of electric machines. However, for a precise topology description, a further differentiation must be made regarding the mounting of the electrical machine. If the machine is mounted on the vehicle chassis, and thus part of the sprung mass, we refer to the topology as (dual) central. If the machine is integrated into the axle, and thus part of the unsprung mass, the topology is marked as eAxle. This definition is independent of the number of machines because eAxle topologies with one (central) or two (dual central) electric machines exist. Because distributed or hub motors are unsprung mass by design, they are also referred to as eAxles [15]. Consequently, our case study defines six topologies for the powered axles (Figure 1). Although technically possible, to our knowledge, no multiple gear eAxle exists, and thus this study focuses on the remaining five.

To extend the knowledge from Verbruggen et al. generic approach, we evaluate the topologies from the perspective of currently available or announced vehicles or driven axles. On the one hand, this shows current development trends in the industry and, on the other hand, provides insights on future optimization potential.

All topologies could also be utilized in  $6 \times 4$  vehicles. However, in this paper, we focus on European trucks and thus  $4 \times 2$  configurations. Due to the different number of EMs, it is technically possible to use differently sized motors and consequently influence the operating points of the EM to optimize vehicle performance such as the Tesla Model 3 [16]. Furthermore, this allows for lateral torque distribution found to be beneficial for energy consumption [17] without sacrificing safety and stability with the correct control strategies [18]. However, to the authors' knowledge, there is currently no heavy-duty vehicle concept utilizing this topology.

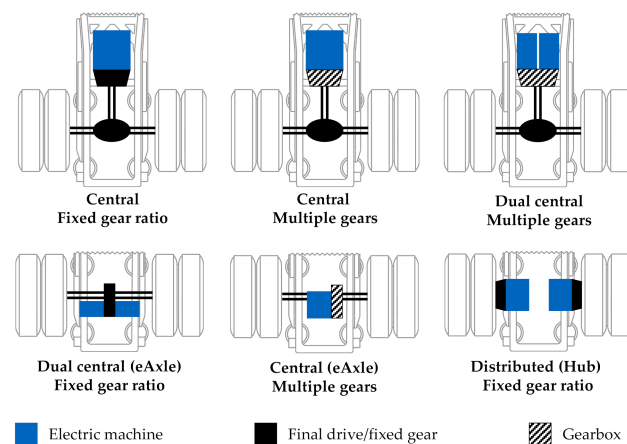


**Figure 1.** Topologies for electric drive axles for heavy-duty trucks.

Verbruggen et al. [14] performed a discrete topology optimization to assess the total cost of ownership as well as energy consumption of feasible topologies. Expanding on their work, we perform a simulative case study with existing vehicles. In addition, we use detailed models to calculate electric machine maps. In contrast to Verbruggen et al., we perform an electric machine design process for each studied configuration. Although this increases the number of input parameters, we assume that we increase overall accuracy with our approach. Furthermore, we test the results' robustness with multiple driving cycles. To test the sensitivity regarding the gearbox design and the associated assumptions, we perform a variation of the overall gearbox ratio and its effect on efficiency and driving performance. In the following, we describe the simulative analysis of the presented topologies and compare them regarding their efficiency.

### 1.2. Electric Machine Efficiency

As an electro-mechanical energy converter, an electric machine is subject to losses [19]. Kremser differentiates three types of losses: (1) load-dependent (e.g., copper), (2) load-independent (e.g., iron or mechanical) losses [20], and (3) additional losses, which can be categorized either as load-dependent or independent [21].

Every machine has operating points with higher and lower efficiency that depend on numerous machine parameters. Determined by the machine type, this choice strongly correlates with the intended application. For example, applications close to the rated speed and higher torque perform better with permanent-magnet synchronous machines (PMSM), whereas induction machines (IM) have better efficiency at higher speeds [16,22].

Due to the required high start-up torque but low-speed requirements in heavy-duty trucks, the electric machine design needs to be adapted compared to passenger electric vehicles [23]. In regard to the dimensions of the machine, this results in a large stator outer diameter and small active length, giving the machine a “disc-like” shape, [24,25]. Due to the incurred high magnetizing currents in an IM and the high resulting excitation losses for synchronous machines but high-efficiency areas of PMSM for high-torque and low-speed applications, a PMSM is usually preferred. High-torque machines are usually established using a lower pole count of  $p = 2-5$  than in regular passenger electric vehicles [24,26]. The ratio between the maximum and rated rotational speed is 1.75–4.4 [27].

## 2. Methodology

For the analysis in this paper, existing electric machines in heavy-duty trucks (40 t gross vehicle weight) in production or prototype stage were summarized. Besides publicly available vehicle parameters, we present our assumptions regarding the gearbox design and the resulting operating speed of the electrical machine. Based on the vehicle parameters, the machine efficiency maps are calculated. To determine average vehicle efficiency, energy

consumption, and driving performance, the efficiency maps are fed into a longitudinal simulation model. Depending on the driving cycle, the resulting operating points and thus efficiency can be derived. The download links to the machine design tool MEAPA and the longitudinal simulation LOTUS are given as Supplementary Material.

### 2.1. Vehicle Parameters

Existing heavy-duty electric trucks and respective electric powertrains currently on the market are summarized in Table 1 regarding their powertrain topology parameters. The topology, number of gears and machines, as well as the machine type, power, and torque, are taken from the respective sources, whereas the rotational velocity of the machine  $n_{85, rated}$  for a maximum vehicle velocity of 85 km/h is calculated using Equations (1) and (2).

$$n_{85, rated} = \frac{85 \frac{km}{h} \cdot \frac{60}{3.6}}{2 \cdot \pi \cdot r_{dyn}} \cdot i_{gear} \quad (1)$$

$$i_{gear} = \frac{35000 Nm}{(No. of machines) \cdot (max torque)} \quad (2)$$

where  $r_{dyn}$  represents the dynamic rolling radius of the tires and  $i_{gear}$  is the gear ratio. The 35,000 Nm represents the startup torque necessary for 40 t heavy-duty trucks. This allows for typical road acceleration ( $>0.646 \text{ m/s}^2$ ) and provides sufficient torque reserves enabling starting on roads with a gradient of 15–17% [11,28,29].

**Table 1.** Summary of heavy-duty trucks or axles of various manufacturers and their respective powertrain topology parameters. **Bold** concepts are simulated in this study. Empty fields indicate unknown information. (Note: EM: electrical machine; PMSM: permanent magnet synchronous machine; IM: induction machine).

Concept	Topology	Gear	No. of Machines	Machine Type	Power (Rated)	Rot. Velocity (Rated) <sup>1</sup>	EM Torque (Max)	Source
Axletech EPS785	central motor	1	1	PMSM <sup>2</sup>	350	-	3500	[30]
<b>DAF CF Electric</b>	<b>central motor</b>	<b>1</b>	<b>1</b>	<b>PMSM</b>	<b>210</b>	<b>8837</b>	<b>2000</b>	<b>[31,32]</b>
Scania L	central motor	1	2	-	230	-	1300	[33]
Hyundai XCIENT	central motor	1	6	-	350	-	3400	[34]
Meritor 17xe	central motor, eAxle	2–3	1	-	410	-	2000	[35]
<b>ZF AxTrax</b>	<b>distributed</b>	<b>1</b>	<b>2</b>	<b>IM</b>	<b>60</b>	<b>11,362</b>	<b>485</b>	<b>[13,36,37]</b>
Nikola Two	distributed	1	4	-	186.25	-	677.75	[38]
<b>Tesla Semi</b>	<b>distributed</b>	<b>1</b>	<b>4</b>	<b>PMSM</b>	<b>223</b>	<b>5700</b>	<b>380</b>	<b>[39]</b>
<b>E-Force EF18 SZM</b>	<b>dual central motor</b>	<b>3</b>	<b>2</b>	<b>PMSM</b>	<b>150</b>	<b>2525</b>	<b>2025</b>	<b>[40–42]</b>
Alisson AXE	dual central motor	2	2	-	400	-	-	[43,44]
Ansorge Elias	dual central motor	12	2	PMSM	140	-	1250	[45]
<b>Nikola Tre</b>	<b>dual central motor, eAxle</b>	<b>1</b>	<b>2</b>	<b>PMSM</b>	<b>240</b>	<b>9819</b>	<b>900</b>	<b>[46–48]</b>

<sup>1</sup> Calculated values using Equations (1) and (2).

For the results in this paper, the electric trucks indicated in bold type in Table 1 were utilized. They were chosen as examples since they represent a reasonable variety of topologies using 1, 2, and 4 electric machines, as well as a combination of fixed and multiple gears. Here, the powertrain topologies in Figure 1 were considered. In order to represent the central fixed gear, the DAF CF electric powertrain was chosen with an implemented PMSM as an electric machine. For the dual central, multiple gear topology,

the E-Force EF18 SZM was chosen, also using a PMSM. The Ansoerge Elias vehicle concept has the same topology but is not commercially available and consequently not included. The Meritor 17xe is an example of a central motor with multiple gears, and it is currently not implemented in a series truck. However, this concept could not be considered because the machine type is unknown. The dual central fixed gear topology is represented by the Nikola Tre using a PMSM for traction and the distributed fixed gear topology by the Tesla Semi with a PMSM. The ZF AxTrax shares the topology with the Tesla Semi, but it is the only concept integrating an IM.

## 2.2. MEAPA Tool

In previous works, the authors presented a holistic, automated design model for IM and PMSM [49,50]. After selecting the machine type, the rated power, rated rotational velocity, rated voltage, and the number of pole pairs need to be defined. In a further step, assumptions in regard to the power factor, number of phases, magnet arrangement, circuit connection, cooling, material selection, and winding layout need to be made. After the machine dimensions are determined, the stator and rotor design continue. Consequently, based on the design parameters, the tool computes valid currents and voltages with separate motor and generator loss models, resulting in the efficiency diagram [49].

In the conducted analysis, the calculated efficiency diagrams were created using the following assumptions in Table 2. The voltage level of 800 V was implemented, since this voltage level is used in the electric trucks from DAF and Nikola [46]. Since the number of pole pairs is not known for the chosen trucks, a value of 4 was chosen since lower pole pair numbers are usually applied for low-speed and high-torque applications [26]. The maximum rotational velocity was set to approximate  $1.75 n_N$  [27].

**Table 2.** Assumptions of input parameters for the machine design tool MEAPA (Note: rpm: revolutions per minute).

Parameter	Symbol	Value	Unit
Voltage (rated)	U	800	V
Number of pole pairs	p	4	-
Rot. velocity (max)	$n_{max}$	$1.75 n_N$	rpm
Power factor	$\cos \varphi$	1	-
Number of phases	m	3	-
Magnet arrangements	-	internal, embedded	-
Circuit-wiring	-	Star	-
Wire-type	-	Round-wire	-
Cooling type	-	Liquid	-
Iron material	-	VACOFLUX50	-
Conductor material	-	Copper	-
Winding type	-	Single-layer, integral-slot	-

Since the power factor and number of phases, as well as circuit-wiring and wire type, were not known from the manufacturers, they were set to the respective values. The magnet arrangement was set to an interior permanent-magnet synchronous machine (IPMSM) with an embedded rotor magnet arrangement, due to the low-speed application [19,25]. A limitation of the machine design tool was reached for the DAF powertrain, since this is usually operated using 9 phases. In order to compare the results to the remaining trucks, a 3-phase topology was applied to all regarded electric machines.

## 2.3. LOTUS

The longitudinal simulation (LOTUS) [51] calculates the energy consumption and the efficiency for each vehicle configuration. The tool allows different powertrain designs and user-defined vehicle parameters. The input parameters and the vehicle weight for this study are based on the values by Fries et al. [52,53] and summarized in Table 3. In accordance with the European commercial vehicle certification tool VECTO, the payload

is set to 19.3 t [54]. All vehicles are equipped with a net battery capacity of 640 kWh (depth-of-discharge of 80%), which is sufficient for most long-haul applications [12]. In addition, the simulation constrains the maximum possible current per machine to 500 A to exclude impractically large diameters of the cables due to cost and weight reduction.

**Table 3.** Assumptions of input parameters for vehicle simulation [52,53].

Parameter	Symbol	Value	Unit
Payload	$m_{payload}$	19,300	kg
Frontal area	$A$	10.2	m <sup>2</sup>
Drag coefficient	$c_W$	0.53	-
Tire radius	$r_{dyn}$	0.4465	m
Rolling drag coefficient	$c_R$	0.0043	-
Auxiliary consumers	$P_{aux}$	3.5	kW

The electric machine weight is calculated based on a linear regression model [55] and shown in Table 4. Because the weight only depends on the machine type and the power, no correlation between weight and topology can be seen. While the battery dominates the total vehicle weight [12], the machine weight comprises 2–6% of the total gross vehicle weight if 40 t payload is assumed.

**Table 4.** Weight of the electrical machines based on a linear regression model [55].

Vehicle	Weight in kg
E Force	1437
ZF	681
Nikola	2345
Tesla	1265
DAF	2118

Besides the electric machine, losses in the powertrain occur in all gearings. We assume an efficiency of 99% for all fixed-gear configurations as well as the highest gear. Lower gears and planetary gears have an efficiency of 96%, while the final drive has an efficiency of 97% [14,53]. These losses account for all losses in the transmission caused by gearing, friction, and oil [13]. The model neglects further losses such as battery charging as they are not affected by the topology or the machine design.

To simulate topologies with a different number of electric machines, the total vehicle torque is divided by the number of machines. The operating points are simulated using efficiency diagrams, as described in Section 2.2. The output torque of a single machine is then multiplied again by the number of EM and, together with the gear ratios, yields the drive torque at the wheel. The required current is also multiplied by the number of EMs and applied to the battery. Consequently, only one machine is simulated to reduce complexity and computation time. However, this implies that all machines provide an equal amount of torque and that lateral torque distribution is neglected.

The input for LOTUS is a driving cycle. For this study, one real-world-based and three synthetic driving cycles are used. The cycles are shown in Figure 2. The first cycle, *Truckerrunde*, is used by the technical journal *Trucker* to evaluate different heavy-duty vehicles. The roundtrip in southern Germany includes highway sections (80 km/h) and rural roads (60 km/h) [56]. The average velocity of the 400 km long test cycle is 75 km/h with a maximum road gradient of 5.2%. Although this cycle is based on a real road profile, the version used does not include any stops. The second and third cycles are driving cycles included in the VECTO tool and used for emission certification by the European Union [57]. The long haul (LH; Figure 2b) has a higher average velocity of 83 km/h compared to the regional delivery driving cycle (RD; Figure 2c) with 66 km/h. In contrast to the *Truckerrunde*, both VECTO cycles include stops of varying length. However, the

average road gradient is lower compared to the *Truckerrunde* cycle (LH: 6.6% and RD: 6.2%). With a total stopping time of 67 s over 2 stops, the long-haul cycle represents a stationary load. The regional delivery cycle has a more dynamic profile with 11 stops and a total stopping time of 746 s. Both VECTO cycles are synthetic cycles, based on real-world driving data. The last assessed driving cycle also represents real-world data synthesized with a Markov-chain approach by Fries et al. [58]. With an average velocity of 73 km/h and no stops, this cycle is comparable to the *Truckerrunde* cycle, although it has a maximum gradient of 6.8%. All synthetic cycles cover a distance of 100 km.

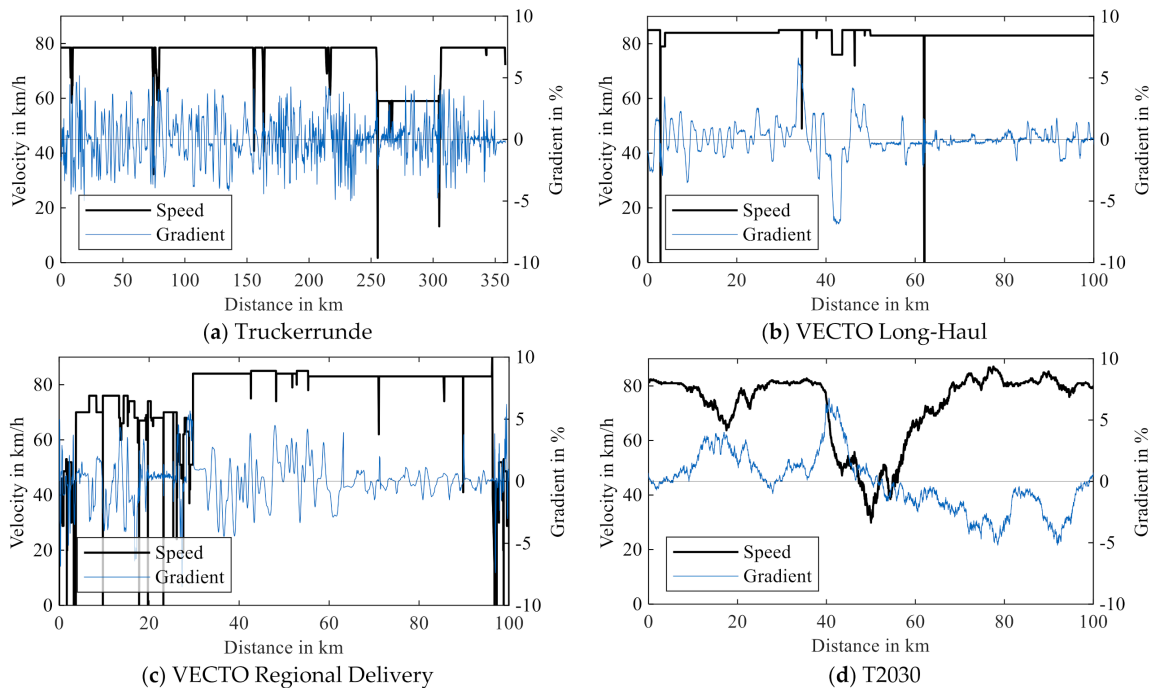


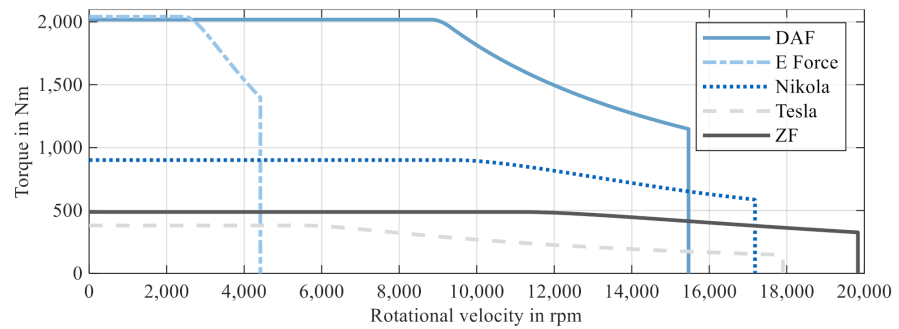
**Figure 2.** Speed profile and road gradient of different driving cycles (a–d). *Truckerrunde* is based on a real road-profile, while the other driving cycles are synthetic driving cycles based on collected and processed driving data.

### 3. Results

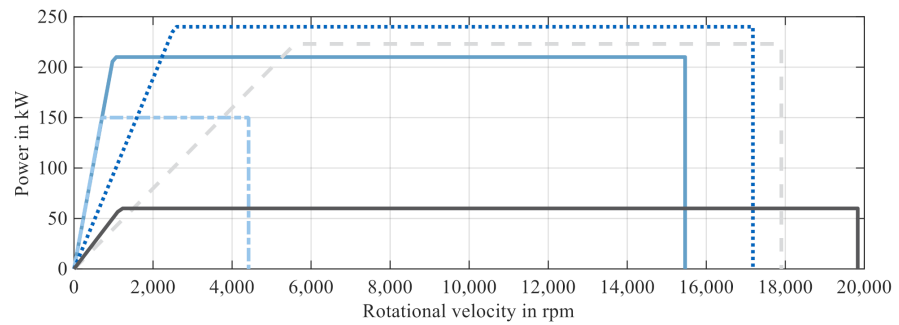
The results of the conducted simulation of the machine design are illustrated in form of the maximum torque vector and the maximum power of each regarded electric machine in Figure 3. The electric machine design for the DAF and E-Force powertrain show the highest torque of the respective concepts, while the E-Force and Tesla provide the highest power. Both the DAF and E-Force are equipped with one and two PMSMs, respectively. A PMSM is implemented in this case in order to offer the necessary high torque.

The different maximum rotational velocities of the powertrain concepts show the impact of the number of gear ratios. While the powertrains of the DAF, Nikola, ZF, and Tesla truck are all equipped with fixed gears, the respective electric machine needs to be designed with a higher rated rotational velocity in order to enable the necessary wheel speed at a variety of driving speeds.

In order to illustrate the operating points of each of the regarded powertrain topologies, LOTUS was utilized as described in Section 2.3. The resulting efficiency diagram displaying the respective operating points for propulsion (positive ordinate) and recuperation (negative ordinate) can be seen in Figure 4. The given average efficiency of the vehicles has a standard deviation of 3.5%.



(a) Maximum torque



(b) Maximum power

**Figure 3.** Curves of the maximum motor torque (a) and the power (b), measured at the output of the electrical machines. The maximum power is limited to the rated power due to technical restriction of the maximum possible current (500 A).

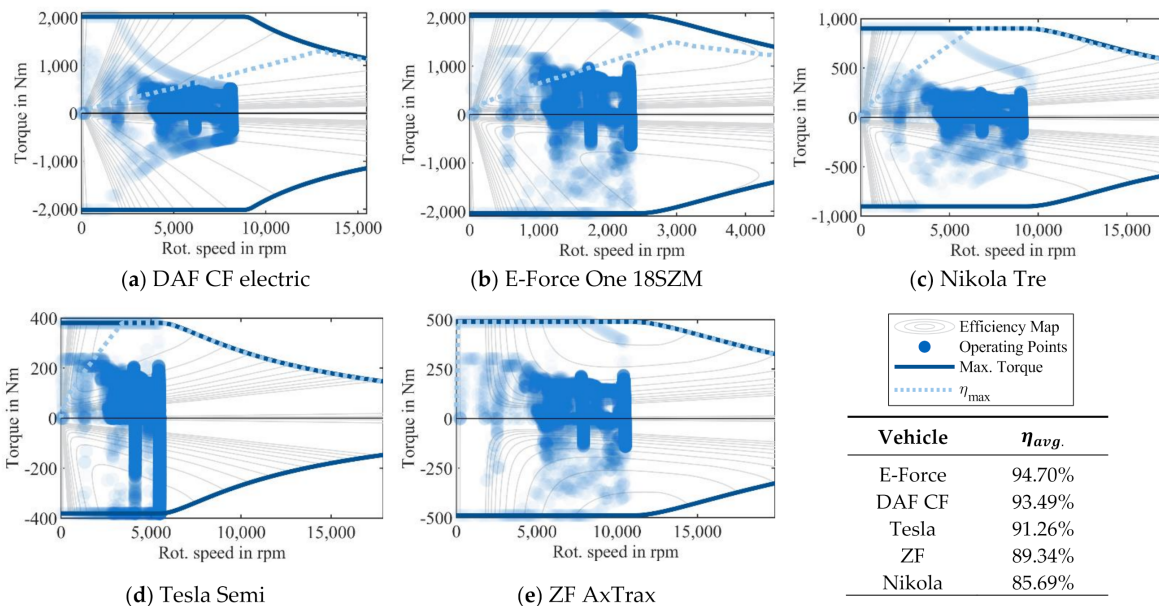


**Figure 4.** Simulation results of operating points, maximum, and average efficiency for regarded electric truck concepts (a–e) during the *Truckerrunde* driving cycle. The hyperbolic shapes are caused by the technical, maximum current of 500 A.

The diagrams show that the operating points are located primarily at the vertical lines that represent the rotational speed around 80 km/h and 60 km/h, respectively. All concepts show most of the operating points near the rated rotational speed and thus at 85 km/h. This confirms the assumption made regarding the gear ratios.

The diagram of the E-Force One (Figure 4b) clearly shows that operating points with lower speeds are present due to shifting. Consequently, the E-Force One powertrain offers the greatest potential to utilize the entire efficiency map due to the multiple-gear topology, and the overall efficiency during real operation is the best out of the regarded topologies.

Because the Nikola Tre's high system torque and power are distributed over two machines, the operating points are located in areas with low torque demand but also low efficiency near the abscissa (Figure 4c). Therefore, the concept shows the lowest efficiency of all vehicles.

The Tesla Semi (Figure 4d) makes full use of the diagram of the EM in both directions. The load on the Tesla machines is relatively high. In contrast, the DAF (Figure 4a) only uses a fraction of the diagram due to the limitation of the maximum current. Thus, the machine could be downsized and designed with a lower-rated rotational speed. The fixed-gear concept implemented in the ZF (Figure 4e) utilizes the entire efficiency diagram despite the lack of shiftable gears, even in high-torque areas.

In general, the multiple-gear box concept of the E-Force offers an advantage of 1.3–9.3% compared to the other topologies. However, the central fixed gear motor topology offers a similar overall efficiency and should therefore not be neglected.

Besides the average efficiency, Figure 5 shows the energy consumption of each vehicle for the four driving cycles. This confirms that within the same driving cycle, the standard deviation for consumption and efficiency is low (4%) for three driving cycles.

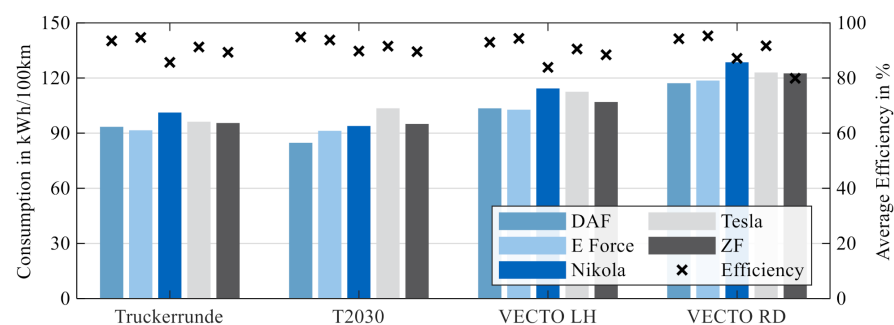


**Figure 5.** Varying driving cycles with different characteristics have an influence on energy consumption and average electric machine efficiency. While Truckerrunde and T2030 do not include stops, both VECTO cycles include multiple stops with varying times (LH: 67 s and RD: 746 s). The spreadsheet containing the results is provided as Supplementary Material.

As the average efficiency is determined by the position of the operating points in the machine map, we investigate how different driving cycles affect the operating points and consequently the efficiency. Thus, the mean value represents both recuperation and propulsion. Consequently, the energy consumption must not necessarily be correlated with the average efficiency, because the latter does not consider the location of the operating point above or below the ordinate. Furthermore, it must be noted that all vehicles recuperate the maximum possible electrical energy. However, if the brake maneuver requires energy beyond that limit, the conventional friction brakes decelerate the vehicle. This means that a high efficiency can be superimposed by conventional braking due to electrical limitations and resulting in higher overall consumption or vice versa. On the one hand, this explains why the Tesla has a high consumption despite high efficiency during the T2030 and the VECTO LH cycle, as both require extensive braking during downhill sections. On the other, the ZF seems to exploit recuperating during the VECTO RD cycle, resulting in relatively low consumption despite low efficiency.

Both central drive topologies have lower energy consumption compared to wheel-independent topologies. The DAF CF has the lowest average consumption over all driving cycles (100 kWh/100 km) followed by E-Force (101 kWh/100 km) and ZF (105 kWh/100 km). The Tesla Semi (109 kWh/100 km) and the Nikola Tre (110 kWh/100 km) pow-

ertrain perform the worst. Although the driving cycles result in different dynamics, we cannot conclude that multi-speed gearboxes have advantages within the selected driving cycles and the different vehicles.

Although all distributed topologies perform worse than the central ones, the ZF results in the regional-delivery cycle—being the most dynamic driving cycle—standing out. The results suggest that the machine design is better suited for this application, which we can assume valid given the machine’s usual application in passenger vehicles.

Comparing the different machine designs, the results show that high-torque machines perform best regarding efficiency and consumption. The advantage regarding consumption becomes less pronounced as the dynamics of the drive cycle increase, suggesting that smaller machines are better suited for the application.

#### 4. Sensitivity Analysis

Besides the driving cycle, the transmission design and foremost the overall gear ratio have an influence on the operating points and thus the efficiency. To test the robustness of our assumptions, we therefore varied the overall ratio in the range of  $\pm 20\%$  from the calculation in Equation (2). Because the VECTO driving cycle showed a consistent relation between high efficiency and low consumption, it was used for this computation. Furthermore, current European vehicle certification utilizes this cycle, which is why we assume these results are easily comparable. The elasticity test was performed without any gradient. The results (Figure 6a,b) show a linear relation between lower gear ratios and higher average efficiency.

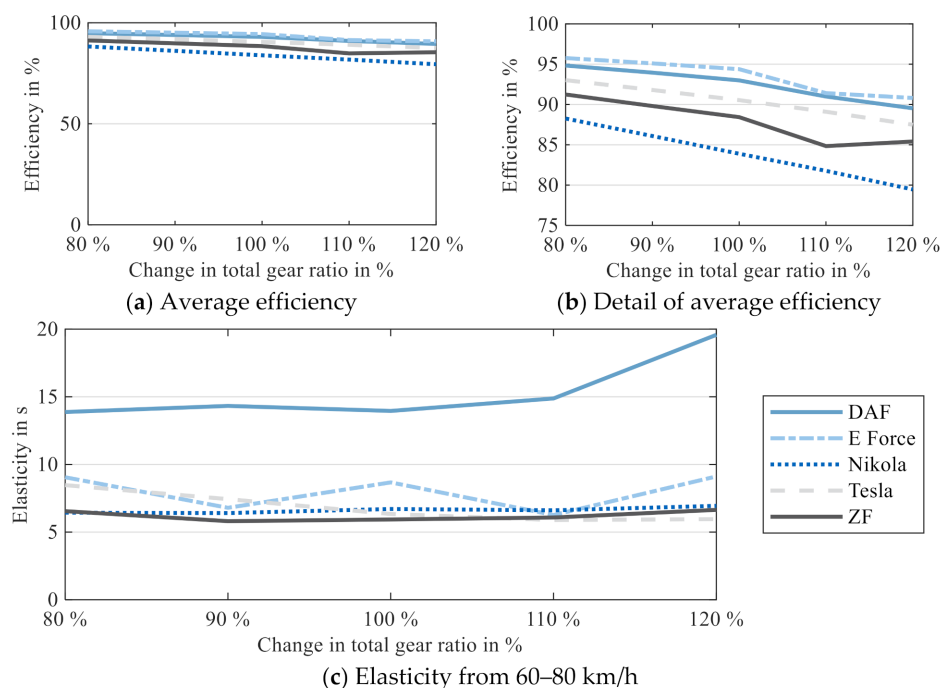


**Figure 6.** The sensitivity of the average electric machine efficiency (a,b) to the change in gear ratio shows a linear decrease in efficiency with higher gear ratios. As a measure for driving performance, the elasticity (c) describes the acceleration time from 60–80 km/h. Its sensitivity to the change in gear ratio shows that smaller ratios increase the elasticity except for the DAF concept. The VECTO LH cycle was used for all simulations. The spreadsheet containing the results is provided as Supplementary Material.

However, the improved efficiency with lower ratios comes at the cost of worse driving performance. As a measure for driving performance, Figure 6c shows the non-linear correlation of the elasticity—the time to accelerate from 60 to 80 km/h—and the gear ratio change. A 20% reduced gear ratio worsens the elasticity up to 34% in the case of

the Tesla. However, an increase in gear ratio (meaning worse efficiency) results in smaller or no improvements in elasticity. The DAF CF shows a different behavior, which can be explained with the constrained maximum current of 500 A. Higher gear ratios cause this limit to be reached earlier and thus reduce the acceleration performance. Although this applies to all vehicles, the impact on the DAF is highest. Due to the oversized torque and power reserves, the DAF and Nikola concept could be optimized regarding efficiency without sacrificing the elasticity. Averaged over the four driving cycles, the low ratio DAF performs best (95.4%), while Nikola (90.1%) outperforms the ZF. The same would hold true for the ZF AxTrax; however, the gear ratio is known [13] and consequently not optimized in this study.

The sensitivity analysis confirms that both central topologies perform better than the concepts with hub or eAxle topologies. Altogether, we conclude that our assumptions regarding the gearbox ratios and design are sufficiently accurate, as the efficiency cannot be improved without worsening driving performance by 4–34%. Although lower gear ratios optimize the DAF and Nikola concepts, they do not alter the general conclusions drawn.

## 5. Discussion

The sensitivity analysis is contradictory to the results presented by Verbruggen et al. [14], who showed the superiority of distributed topologies and the additional advantage of multi-speed gearboxes regarding energy consumption and thus efficiency. However, we assume the vehicles in this study were not optimized in the same way as Verbruggen et al. were. Including the machine design in our approach, we show that the choice of machine design and topology can influence the overall efficiency in the same range as the choice of topology, as Verbruggen et al. showed. Consequently, we conclude that an optimized battery electric truck requires both the optimum topology and the optimum machine design.

The longitudinal simulation was carried out for a single machine, whose output torque was multiplied by the respective number of machines in the topology. Consequently, lateral torque distribution as neglected. Finken et al. [16] showed the potential of optimizing the lateral torque distribution to maximize the overall efficiency. A combination of different types or sized machines could further optimize the efficiency. A combination of different types or sizes of machines could further optimize efficiency. For example, Tesla offers its Model 3 as a four-wheel-drive with a PMSM on the front and an IM on the rear axle. Depending on the load, either one or both drive the car in order to provide maximum efficiency in all situations. At higher speeds, the IM primarily propels the car, while at lower speeds the PMSM takes over. As both machines have efficiency advantages in the respective ranges, efficiency and range improve [16]. This could also be considered in future studies for heavy-duty applications; however, none of the currently known prototypes provide this technology.

A limitation of this study is that only the gear ratios of the ZF AxTrax system are known. The other ratios were assumed such that rated rotational speed matches the vehicle's legal speed on European highways. If different ratios are chosen, the results could differ significantly. Furthermore, the assumed shifting rules try to keep the rotational speed in the range of  $0.2 n_N$  and  $0.8 n_{max}$ . As the real shifting rules are unknown, this assumption cannot be verified.

In addition, the validation of the part models needs to be discussed. Since the electric machine design tool used for the creation of the efficiency diagrams is mainly validated for parameter ranges of passenger vehicles, high-torque machines pose a simulation area that could not be validated to date. However, the resulting diagrams were verified by comparing similar high-torque applications such as electric busses. In future studies, the impact of the number of phases on the performance of the concept could be further investigated, since the DAF electric machine has a nine-phase instead of the implemented three-phase topology.

The examined concepts are not in series production yet. Thus, fleet data could not be collected, nor were test data publicly accessible. However, LOTUS is validated for conventional ICE-powered vehicles [59]. Since the vehicle model and remaining components are unchanged, we assume the results to be plausible and valid within the given limitations. However, as the presented study compares the topologies relatively to each other, the general conclusions are plausible. Future studies should consider the optimization of gear ratios and shifting rules depending on the topology and electric machine design.

## 6. Conclusions

In this paper, we investigated the influence of the powertrain topology in the combination of electric with machine design on the vehicle efficiency operation. The results show that due to the topology, averaged efficiencies range between 87% and 95%. Our results show that the single central topology shows the highest overall efficiency and lowest consumption. However, the applications' effect (i.e., driving cycles) superimposes this conclusion and yields consumptions in a range between 93–122 kWh/100 km. Furthermore, the application can result in low consumption despite low efficiency, as the ZF concepts show during the VECTO RD cycle.

On the one hand, we show that current concepts are far from the optimal solutions presented by Verbruggen et al [14]. On the other hand, our results highlight that future approaches must not only consider the powertrain topology. Only an application-specific machine design combined with an optimized topology can realize the full potential of electric trucks.

Furthermore, we expect our findings to become more relevant, considering future energy sources. In particular, hydrogen-powered vehicles require the optimization of the complete powertrain to counteract the lower fuel-cell efficiency. However, regardless of the energy source, the cost-sensitive transportation sector requires all technical levers to be pulled to optimize efficiency, energy consumption, and ultimately lower transport emissions.

**Supplementary Materials:** The following are available online at <https://www.mdpi.com/1996-1073/14/2/328/s1>, Both the LOTUS vehicle consumption model and the electric machine design tool MEAPA are available as open source Matlab/Simulink code on Github [51,60]. In addition, the data presented in Table 1 as well as the derived machine design parameters are available as supplementary information. The spreadsheet is available online at INSERT LINK.

**Author Contributions:** Conceptualization, S.W. and S.K.; methodology, S.W. and S.K.; software, S.W., S.K., and M.B.; validation, S.W., S.K., and M.B.; formal analysis, S.W. and S.K.; investigation, S.W., S.K., and M.B.; resources, M.L.; data curation, S.W., S.K., and M.B.; writing—original draft preparation, S.W. and S.K.; writing—review and editing, S.W., S.K., M.B., and M.L.; visualization, S.W. and M.B.; supervision, M.L.; project administration, M.L.; funding acquisition, M.L. All authors have read and agreed to the published version of the manuscript.

**Funding:** This research received no external funding. The research of S. W. was funded by basic research funds of the Institute of Automotive Technology. The research of S. K. was supported by the organization Bayern Innovativ and the Bavarian Ministry of Economic Affairs, Regional Development and Energy within the research project DeTailED—Design of Tailored Electrical Drivetrains.

**Institutional Review Board Statement:** Not applicable.

**Informed Consent Statement:** Informed.

**Data Availability Statement:** The data presented in this study are openly available in the repositories LOTUS at 10.13140/RG.2.2.27745.53607 and MEAPA at [https://github.com/TUMFTM/Electric\\_Machine\\_Design](https://github.com/TUMFTM/Electric_Machine_Design). The data displayed is provided as supplementary material.

**Conflicts of Interest:** The authors declare no conflict of interest.

## Abbreviations

The following abbreviations are used in this manuscript:

BEV	Battery Electric Vehicle
EM	Electric Machine
EU	European Union
FCEV	Fuel Cell Electric Vehicle
ICE(V)	Internal Combustion Engine (Vehicle)
IM	Induction Machine
IPMSM	Interior Permanent-Magnet Synchronous Machine
LH	Long Haul
LOTUS	Long-Haul Truck Simulation
MEAPA	Model for the design and analysis of a PMSM or ASM (German: Modell für den Entwurf und die Analyse einer PMSM oder ASM)
PMSM	Permanent-Magnet Synchronous Machine
RD	Regional Delivery
VECTO	Vehicle Energy Consumption Calculation Tool

## References

- Paris Agreement—Climate Action—European Commission. Available online: [https://ec.europa.eu/clima/policies/international/negotiations/paris\\_en#tab-0-0](https://ec.europa.eu/clima/policies/international/negotiations/paris_en#tab-0-0) (accessed on 1 August 2019).
- European Environment Agency. *Greenhouse Gas Emissions from Transport in Europe*; EEA: Copenhagen, Denmark, 2019; Available online: [https://www.eea.europa.eu/ds\\_resolveuid/7009a89effc04d8ea8b5f94ff0a39912](https://www.eea.europa.eu/ds_resolveuid/7009a89effc04d8ea8b5f94ff0a39912) (accessed on 23 April 2020).
- Regulation of the European Parliament and of the Council Setting CO<sub>2</sub> Emission Performance Standards for New Heavy-Duty Vehicles, 2018.
- Moultak, M.; Lutsey, N.; Hall, D. Transitioning to Zero-Emission Heavy-Duty Freight Vehicles. 2017. Available online: <https://theicct.org/publications/transitioning-zero-emission-heavy-duty-freight-vehicles> (accessed on 14 December 2018).
- Wallentowitz, H.; Freialdenhoven, A.; Olschewski, I. *Strategien zur Elektrifizierung des Antriebsstranges. Technologien, Märkte und Implikationen (Strategies for Powertrain Electrification: Technologies, Markets and Implications)*; Vieweg + Teubner/GWV Fachverlage GmbH: Wiesbaden, Germany, 2010; ISBN 9783834897015.
- Cano, Z.P.; Banham, D.; Ye, S.; Hintennach, A.; Lu, J.; Fowler, M.; Chen, Z. Batteries and fuel cells for emerging electric vehicle markets. *Nat. Energy* **2018**, *3*, 279–289. [[CrossRef](#)]
- Nicoletti, L.; Bronner, M.; Danquah, B.; Koch, A.; König, A.; Krapf, S.; Pathak, A.; Schockenhoff, F.; Sethuraman, G.; Wolff, S.; et al. Review of Trends and Potentials in the Vehicle Concept Development Process. In Proceedings of the 2020 Fifteenth International Conference on Ecological Vehicles and Renewable Energies (EVER), Monte-Carlo, Monaco, 10–12 September 2020; pp. 1–15, ISBN 9781728156415.
- Mahmoudi, A.; Soong, W.L.; Pellegrino, G.; Armando, E. Efficiency maps of electrical machines. In Proceedings of the 2015 IEEE Energy Conversion Congress and Exposition (ECCE 2015), Montreal, QC, Canada, 20–24 September 2015; IEEE: Piscataway, NJ, USA, 2015; pp. 2791–2799, ISBN 9781467371513.
- Mareev, I.; Becker, J.; Sauer, D. Battery Dimensioning and Life Cycle Costs Analysis for a Heavy-Duty Truck Considering the Requirements of Long-Haul Transportation. *Energies* **2018**, *11*, 55. [[CrossRef](#)]
- Sen, B.; Ercan, T.; Tatari, O. Does a battery-electric truck make a difference?—Life cycle emissions, costs, and externality analysis of alternative fuel-powered Class 8 heavy-duty trucks in the United States. *J. Clean. Prod.* **2017**, *141*, 110–121. [[CrossRef](#)]
- Hoepke, E.; Appel, W.; Brähler, H.; Dahlhaus, U. *Nutzfahrzeugtechnik*; Springer Fachmedien: Wiesbaden, Germany, 2010; ISBN 9783834809957.
- Wolff, S.; Seidenfus, M.; Gordon, K.; Álvarez, S.; Kalt, S.; Lienkamp, M. Scalable Life-Cycle Inventory for Heavy-Duty Vehicle Production. *Sustainability* **2020**, *12*, 5396. [[CrossRef](#)]
- Naunheimer, H.; Bertsche, B.; Ryborz, J. *Fahrzeuggetriebe. Grundlagen, Auswahl, Auslegung und Konstruktion (Automotive Transmissions. Basics, Selection, Design and Construction)*, 3rd ed.; Springer: Berlin, Germany, 2019; ISBN 9783662588833.
- Verbruggen, F.J.R.; Silvas, E.; Hofman, T. Electric Powertrain Topology Analysis and Design for Heavy-Duty Trucks. *Energies* **2020**, *13*, 2434. [[CrossRef](#)]
- Füßel, A. Entwicklungspotenzial technischer Kriterien der BEV-Technologie. In *Technische Potenzialanalyse der Elektromobilität: Stand der Technik, Forschungsausblick und Projektion auf das Jahr 2025*; Füßel, A., Ed.; Springer Fachmedien Wiesbaden: Wiesbaden, Germany, 2017; pp. 35–82, ISBN 9783658166953.
- Finken, T. Fahrzyklusgerechte Auslegung von Permanentmagneterregten Synchronmaschinen für Hybrid- und Elektrofahrzeuge (Design of Permanent Magnet Excited Synchronous Machines for Hybrid and Electric Vehicles according to the Driving Cycle). Ph.D. Thesis, Technical University of Aachen, Aachen, Germany, 2011.
- Hu, X.; Li, Y.; Lv, C.; Liu, Y. Optimal Energy Management and Sizing of a Dual Motor-Driven Electric Powertrain. *IEEE Trans. Power Electron.* **2019**, *34*, 7489–7501. [[CrossRef](#)]

18. Guo, N.; Lenzo, B.; Zhang, X.; Zou, Y.; Zhai, R.; Zhang, T. A Real-Time Nonlinear Model Predictive Controller for Yaw Motion Optimization of Distributed Drive Electric Vehicles. *IEEE Trans. Veh. Technol.* **2020**, *69*, 4935–4946. [[CrossRef](#)]
19. Teigelkötter, J. *Energieeffiziente elektrische Antriebe: Grundlagen, Leistungselektronik, Betriebsverhalten und Regelung von Drehstrommotoren (Energy-Efficient Electric Drives: Fundamentals, Power Electronics, Operating Behavior and Control of Three-Phase Motors)*; Vieweg + Teubner: Wiesbaden, Germany, 2013; ISBN 9783834823304.
20. Kremser, A. *Elektrische Maschinen und Antriebe (Electrical Machines and Drives)*; Vieweg + Teubner: Wiesbaden, Germany, 2004; ISBN 9783519161882.
21. Müller, G.; Ponick, B. *Berechnung Elektrischer Maschinen (Computation of Electrical Machines)*, 10th ed.; Wiley-VCH: Berlin, Germany, 2014; ISBN 9783527405251.
22. Hofmann, P. *Hybridfahrzeuge (Hybridvehicles)*, 2nd ed.; Springer: Vienna, Austria, 2014; ISBN 9783709117798.
23. Simion, A.; Livadaru, L.; Mihai, S.; Munteanu, A.; Cantemir, C.G. Induction Machine with Improved Operating Performances for Electric Trucks. A FEM-Based Analysis. *Adv. Electr. Comput. Eng.* **2010**, *10*, 71–76. [[CrossRef](#)]
24. Permanent Magnet Synchronous Machines as “Brushless DC Drives”: High Torque Machines. Available online: [https://www.ew.tu-darmstadt.de/media/ew/vorlesungen\\_4/vorlesungmotordevelopmentforelectricaldrivesystems/ss\\_14/Folie\\_MD\\_1\\_5\\_english.pdf](https://www.ew.tu-darmstadt.de/media/ew/vorlesungen_4/vorlesungmotordevelopmentforelectricaldrivesystems/ss_14/Folie_MD_1_5_english.pdf) (accessed on 7 February 2020).
25. Binder, A. *Elektrische Maschinen und Antriebe (Electrical Machines and Powertrains)*, 1st ed.; Springer: Berlin, Germany, 2012; ISBN 9783540718499.
26. Artetxe, G.; Paredes, J.; Prieto, B.; Martinez-Iturralde, M.; Elosegui, I. Optimal Pole Number and Winding Designs for Low Speed–High Torque Synchronous Reluctance Machines. *Energies* **2018**, *11*, 128. [[CrossRef](#)]
27. Grunditz, E.A.; Thiringer, T. Performance Analysis of Current BEVs Based on a Comprehensive Review of Specifications. *IEEE Trans. Transp. Electrific.* **2016**, *2*, 270–289. [[CrossRef](#)]
28. Rafael, M.; Lozano, A.; Cervantes, J.; Mucino, V.; Cajun, C.L. A method for powertrain selection of heavy-duty vehicles with fuel savings. *IJHVS* **2009**, *16*, 49. [[CrossRef](#)]
29. Yang, G.; Xu, H.; Wang, Z.; Tian, Z. Truck acceleration behavior study and acceleration lane length recommendations for metered on-ramps. *Int. J. Transp. Sci. Technol.* **2016**, *5*, 93–102. [[CrossRef](#)]
30. AxleTech. EPS Series. EPS785. 2018. Available online: <https://www.axletech.com/at-admin/resources/Literature/eps785-flyerletterweb.pdf> (accessed on 13 February 2020).
31. DAF Trucks Showcases Electric and Hybrid Trucks at IAA CV. Available online: <https://www.greencarcongress.com/2018/09/20180927-daf.html> (accessed on 13 February 2020).
32. DAF Präsentiert Neuen E-Lkw (DAF Presents New E-Truck). Available online: <https://www.eurotransport.de/artikel/cf-electric-als-6x2-fahrgestell-daf-praesentiert-neuen-e-lkw-10986730.html> (accessed on 13 February 2020).
33. Scania Stellt Vollelektrischen Lkw Mit 250 km Reichweite vor (Scania Introduces All-Electric Truck with 250 km Range). Available online: <https://www.scania.com/ch/de/home/experience-scania/news-and-events/News/archive/2020/09/bev.html> (accessed on 2 December 2020).
34. Hyundai Liefert erste Xcient Fuel Cell Brennstoffzellen-Lkw aus (Hyundai Delivers first Xcient Fuel Cell Fuel Cell Trucks). Available online: <https://www.hyundai.news/de/unternehmen/hyundai-liefert-erste-xcient-fuel-cell-brennstoffzellen-lkw-aus/> (accessed on 2 December 2020).
35. Meritor Introduces Electric Drives for Heavy Trucks—Electrive.com. Available online: <https://www.electrive.com/2019/10/30/meritor-introduces-electric-drives-for-heavy-trucks/> (accessed on 13 February 2020).
36. AxTrax (in Development). Available online: [https://www.zf.com/products/en/trucks/products\\_48386.html](https://www.zf.com/products/en/trucks/products_48386.html) (accessed on 13 February 2020).
37. ZF Friedrichshafen AG. Product Overview. Axle & Transmission Systems for Buses & Coaches. 2019. Available online: [https://www.zf.com/products/media/product\\_media/buses\\_1/product\\_overview\\_1/product\\_overview\\_axle\\_transmission\\_systems.pdf](https://www.zf.com/products/media/product_media/buses_1/product_overview_1/product_overview_axle_transmission_systems.pdf) (accessed on 13 February 2020).
38. Electric Trucks: Complete Disagreement. Available online: <https://www.idtechex.com/ko/research-article/electric-trucks-complete-disagreement/9529> (accessed on 13 February 2020).
39. Here’s Everything We Know about the Tesla Semi. Available online: <https://www.trucks.com/2019/09/05/everything-we-know-about-the-tesla-semi-truck/> (accessed on 13 February 2020).
40. E-Force One AG. Facts & Figures. E-Trucks. 2019. Available online: <https://www.eforce.ch/products/ef26> (accessed on 13 February 2020).
41. BRUSA Supplies Complete Drivetrain for E-FORCE 18-t Electric Truck. Available online: <https://www.greencarcongress.com/2013/07/brusa-20130718.html> (accessed on 13 February 2020).
42. Heerwagen, M. So Wird aus Einem Diesel- ein E-Lkw (How a Diesel Truck Becomes an E-Truck). *Eurotransport*. 4 May 2020. Available online: <https://www.eurotransport.de/artikel/umbau-von-diesel-zu-e-lkw-von-0-auf-800-volt-11160701.html> (accessed on 1 December 2020).
43. Allison Introduces New AXE Series E-Axles for MD, HD Trucks; in Peterbilt 579EV Class 8 EV for Testing. Available online: <https://www.greencarcongress.com/2019/04/20190425axe.html> (accessed on 13 February 2020).
44. Neue E-Achsen von Allison (New E-Axles from Allison). Available online: <https://www.eurotransport.de/artikel/fuer-lkw-und-busse-neue-e-achsen-von-allison-10757781.html> (accessed on 13 February 2020).

45. Elias-E-Truck auf dem Weg in Die Serienfertigung (Elias E-Truck on the Way to Series Production). Available online: <https://transport-online.de/news/elias-e-truck-auf-dem-weg-die-serienfertigung-14533.html> (accessed on 13 February 2020).
46. Robar, C. IVECO, FPT Industrial and Nikola Corporation Unveil the Nikola TRE. 2019. Available online: [https://nikolamotor.com/press\\_releases/iveco-fpt-industrial-and-nikola-corporation-unveil-the-nikola-tre-71](https://nikolamotor.com/press_releases/iveco-fpt-industrial-and-nikola-corporation-unveil-the-nikola-tre-71) (accessed on 13 February 2020).
47. Hoffmann, J. Elektro-Lkw Kommt 2021 (Electric Truck Coming in 2021). *Eurotransport*. 5 December 2019. Available online: <https://www.eurotransport.de/artikel/nikola-tre-auf-iveco-basis-elektro-lkw-kommt-2021-11037980.html> (accessed on 1 December 2020).
48. Inside Nikola's Truck Technology—From Fuel Cells to Lights. Available online: <https://www.trucks.com/2019/05/22/inside-nikolas-truck-technology-fuel-cells-tail-lights/> (accessed on 1 December 2020).
49. Kalt, S.; Erhard, J.; Danquah, B.; Lienkamp, M. Electric Machine Design Tool for Permanent Magnet Synchronous Machines. In Proceedings of the 2019 Fourteenth International Conference on Ecological Vehicles and Renewable Energies (EVER), Monte-Carlo, Monaco, 8–10 May 2019; IEEE: Piscataway, NJ, USA, 2019; pp. 1–7, ISBN 9781728137032.
50. Kalt, S.; Erhard, J.; Lienkamp, M. Electric Machine Design Tool for Permanent Magnet Synchronous Machines and Induction Machines. *Machines* **2020**, *8*, 15. [CrossRef]
51. LOTUS—Long-Haul Truck Simulation: Longitudinal Dynamic Simulation for Heavy Duty Vehicles. Available online: <https://github.com/TUMFTM/LOTUS>. (accessed on 1 January 2021).
52. Fries, M.; Kruttschnitt, M.; Lienkamp, M. Multi-objective optimization of a long-haul truck hybrid operational strategy and a predictive powertrain control system. In Proceedings of the Twelfth International Conference on Ecological Vehicles and Renewable Energies (EVER), Monte-Carlo, Monaco, 11–14 April 2017; pp. 1–7.
53. Fries, M.; Lehmeier, M.; Lienkamp, M. Multi-criterion optimization of heavy-duty powertrain design for the evaluation of transport efficiency and costs. In Proceedings of the 2017 IEEE 20th International Conference on Intelligent Transportation Systems (ITSC), Yokohama, Japan, 16–19 October 2017; IEEE: Piscataway, NJ, USA, 2017; pp. 1–8, ISBN 9781538615263.
54. Tansini, A.; Nikiforos-Georgios, Z.; Prado Rujas, I.; Fontaras, G. *Analysis of VECTO data for Heavy-Duty Vehicles (HDV) CO<sub>2</sub> Emission Targets*; Publications Office of the European Union: Luxembourg, Brussels, 2018. [CrossRef]
55. Fries, M.; Wolff, S.; Horlbeck, L.; Kerler, M.; Lienkamp, M.; Burke, A.; Fulton, L. Optimization of hybrid electric drive system components in long-haul vehicles for the evaluation of customer requirements. In Proceedings of the 2017 IEEE 12th International Conference on Power Electronics and Drive Systems (PEDS), Honolulu, HI, USA, 12–15 December 2017; IEEE: Piscataway, NJ, USA, 2017; pp. 1141–1146, ISBN 9781509023646.
56. So Testet der TRUCKER. Available online: <http://www.trucker.de/so-testet-der-trucker-1156608.html> (accessed on 13 September 2017).
57. Rexeis, M.; Quaritsch, M.; Hausberger, S.; Silberholz, G.; Kies, A.; Steven, H.; Goschütz, M.; Vermeulen, R. VECTO Tool Development: Completion of Methodology to Simulate Heavy Duty Vehicles' Fuel Consumption and CO<sub>2</sub> Emissions. Upgrades to the Existing Version of VECTO and Completion of Certification Methodology to be Incorporated into a Commission Legislative Proposal. 2017. Available online: [https://ec.europa.eu/clima/sites/clima/files/transport/vehicles/docs/sr7\\_lot4\\_final\\_report\\_en.pdf](https://ec.europa.eu/clima/sites/clima/files/transport/vehicles/docs/sr7_lot4_final_report_en.pdf) (accessed on 15 February 2019).
58. Fries, M.; Baum, A.; Wittman, M.; Lienkamp, M. Derivation of a real-life driving cycle from fleet testing data with the Markov-Chain-Monte-Carlo Method. In Proceedings of the 2018 IEEE 21st International Conference on Intelligent Transportation Systems (ITSC), Maui, HI, USA, 4–7 November 2018; IEEE: Piscataway, NJ, USA, 2018.
59. Fries, M.; Sinning, M.; Lienkamp, M.; Höpfner, M. Virtual Truck—A Method for Customer Oriented Commercial Vehicle Simulation. In *Commercial vehicle technology 2016, Proceedings of the 4th Commercial Vehicle Technology Symposium (CVT 2016), 8–10 March 2016, Kaiserslautern, Germany*; Berns, K., Dreßler, K., Fleischmann, P., Ilsen, R., Jörg, B., Kalmar, R., Nagel, T., Schindler, C., Stephan, N.K., Eds.; Shaker Verlag: Herzogenrath, Germany, 2016; ISBN 9783844042290.
60. MEAPA—Model for the Design and Analysis of a PMSM or ASM (German: Modell für den Entwurf und die Analyse einer PMSM oder ASM). Available online: [https://github.com/TUMFTM/Electric\\_Machine\\_Design](https://github.com/TUMFTM/Electric_Machine_Design) (accessed on 1 January 2021).